UDC 532.783

A. Sh. Saidgaziev, A. V. Dubtsov

OCTYLCYANOBIPHENYL LIQUID CRYSTAL CONFINED TO ANISOTROPIC POROUS PET FILMS AT HOMEOTROPIC ANCHORING: OPTICAL TEXTURES AND INTERNAL ORDERING

MIREA – Russian Technological University, Problem Laboratory of Molecular Acoustics,
78 Vernadskogo Pr., Moscow, 119454, Russia. E-mail: alexdubtsov@mail.ru

We report the study of optical textures and internal ordering of homeotropically aligned octylcyanobiphenyl (8CB) liquid crystal, which is characterized by both nematic and smectic phases, confined to porous polyethylene terephthalate films. Taking into account previously reported results, experimental and theoretical data allowed identifying the internal ordering of 8CB within the pores. Despite of completely different spatial ordering, experimental observations revealed similar optical patterns for both liquid-crystalline phases. The presented results can be used in photonic LC applications.

Key words: *liquid crystals, octylcyanobiphenyl, porous film, optical texture, director configuration.*

DOI: 10.18083/LCAppl.2018.4.95

А. Ш. Саидгазиев, А. В. Дубцов

ЖИДКИЙ КРИСТАЛЛ ОКТИЛЦИАНОБИФЕНИЛ, ОГРАНИЧЕННЫЙ АНИЗОТРОПНЫМИ ПОРИСТЫМИ ПЭТ ПЛЕНКАМИ ПРИ ГОМЕОТРОПНОМ СЦЕПЛЕНИИ: ОПТИЧЕСКИЕ ТЕКСТУРЫ И ВНУТРЕННЕЕ УПОРЯДОЧЕНИЕ

МИРЭА – Российский технологический университет, Проблемная лаборатория молекулярной акустики,
пр. Вернадского, д. 78, 119454 Москва, Россия. E-mail: alexdubtsov@mail.ru

Мы сообщаем об исследовании оптических текстур и внутреннего упорядочения гомеотропно ориентированного жидкого кристалла октилцианобифенила (8ЦБ), который характеризуется нематической и смектической фазами, ограниченного пористой полиэтилентерефталатной пленкой. Анализ экспериментальных и теоретических данных с учетом полученных ранее результатов, позволил определить внутреннее упорядочение 8ЦБ внутри пор. Несмотря на различное пространственное упорядочение экспериментальные наблюдения показали схожие оптические текстуры для обоих жидкокристаллических фаз. Полученные результаты могут быть использованы в фотонных ЖК-приложениях.

Ключевые слова: *жидкие кристаллы, октилцианобифенил, оптические текстуры, конфигурация директора.*

Introduction

Liquid crystals (LCs) confined to micrometer-sized curvilinear (non-planar) geometries are attractive from both fundamental and applied points of view [1]. In this case, a strong confinement provides higher sensitivity to the external stimuli and lower switching times, respectively to flat LC layers, which is important at a practical elaboration of new LC devices for sensing [2, 3] and photonic [4] applications. In the simplest case, LC materials comprise micrometer-sized droplets or cylinders surrounded by a polymer matrix. For example, recently porous polymer films filled with LCs were proposed to control a propagation of electromagnetic waves of IR and THz ranges of wavelengths [5, 6].

At the same time, a presence of the strong curvature may induce the formation of complex director configurations characterized by various topological defects, arising in LC phases due to topological conservation laws [7]. Therefore, optical properties of the composite LC materials strongly depend on internal ordering of LC within confining media. Variations of the surface alignment, anchoring strength, elastic parameters of LC and size of the confinement result in different LC structures. Several director configurations were predicted for both nematic and SmA phases within cylindrical cavities [8]. Previously, internal ordering and phase behavior of 8CB (characterized by both nematic and SmA phases) within submicrometer and micrometer cylindrical cavities were studied by the nuclear magnetic resonance [9], calorimetry [10, 11], X-ray [12] and dynamic light scattering [13].

Direct optical observations of 8CB within submillimeter cylindrical cavities treated with a homeotropic surfactant at cooling from nematic to SmA showed a strong difference in optical textures, when light passed along normal to the cylindrical capillary [14]. It was found that escaped radial with point defects (ERPD, see Fig. 1, A) and smectic planar radial (SPR, see Fig. 1, B) configurations were formed for nematic and SmA phases, respectively [14].

In the present study, we analyze optical textures of 8CB confined to porous polymer films at propagation of light along the cylindrical cavities.

Experimental

For this purpose, we used track-etched membranes (Fig. 1, D–F) based on polyethylene terephthalate (PET) films of a thickness h = 23 μm. The membranes contained cylindrical open-end and randomly allocated pores (a diameter d = 5 μm), oriented normally to the film's surface (see Fig. 1, G).

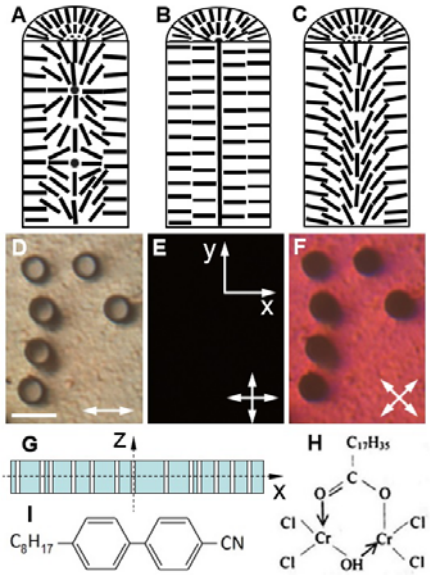

Fig. 1. Sketches of ERPD (A), SPR (B) and ER (C) director configurations. BF (D) and PL (E,F) images of the anisotropic PET film free of LC at various positions respectively to polarizers. A profile of the film (G). Chemical formulas of chromolan (H) and 8CB (I) used in the experiment. Scale bar is 10 μm

The porous films were preliminary treated by chromolan (Fig. 1, H) for homeotropic alignment of LC at the pore walls. The PET films were placed in a handmade hot stage and filled with 8CB (Fig. 1, I) in the isotropic phase. Polarized optical microscopy (POM) with a 1000x magnification was performed to study optical textures of 8CB within the PET films. Polarized light (PL) and bright (BF) fields were used for an observation of the PET-8CB films using a red filter with a peak at λ = 650 nm.

Results and discussion

Figure 2, A–G shows microscopic images of the PET-8CB film after cooling from the isotropic state to the deep nematic phase. In the nematic phase, the 8CB texture revealed a cross-like figure within the pores (Fig. 2, A–G), which was observed independently from positions of the PET-8CB film respectively to crossed polarizers (Fig. 2, D–E). Such behavior revealed the presence of the symmetry axis aligned along the pore's (z) axis. Switching on the full wave plate showed a yellow (blue) color (Fig. 2, F) in quadrants II and IV (I and III), which indicated a homeotropic orientation of a nematic director at the

pore walls. At the same time, BF images (Fig. 2, G) revealed a wide black spot in the center of pores as a result of strong variations of the effective refractive index due to the presence of topological defects or strong curvature in the ER configuration (Fig. 1, C), which possibly induced a waveguide regime. At the same time, variations of the focal plane in the limit of the thickness of the PET-8CB film did not allow to focus at the topological defects (did not show narrowing of the wide black spot to a thinner dot), which indicated a possible absence of the topological defects and formation of the ER structure. The ERPD configuration was established for the mentioned above cylindrical glass capillaries with a submillimeter diameter (200 μm) of pores [14], which was 40 times larger than the diameter of pores used in the present study. Note that the ER configuration was predicted and realized in cylinders with radia $R > 1$ μm. Therefore, our micrometer-sized cylindrical cavities could induce escape of the nematic director to the z axis. The experimental intensity profiles (Fig. 2, H) do not show a large number of the interference stripes in a comparison with the theoretical simulations for the pure ER structure (see Appendix). It can be explained by an overlay of the extremes at light illumination because of small distances between them, which are out of the resolution of optical microscopes.

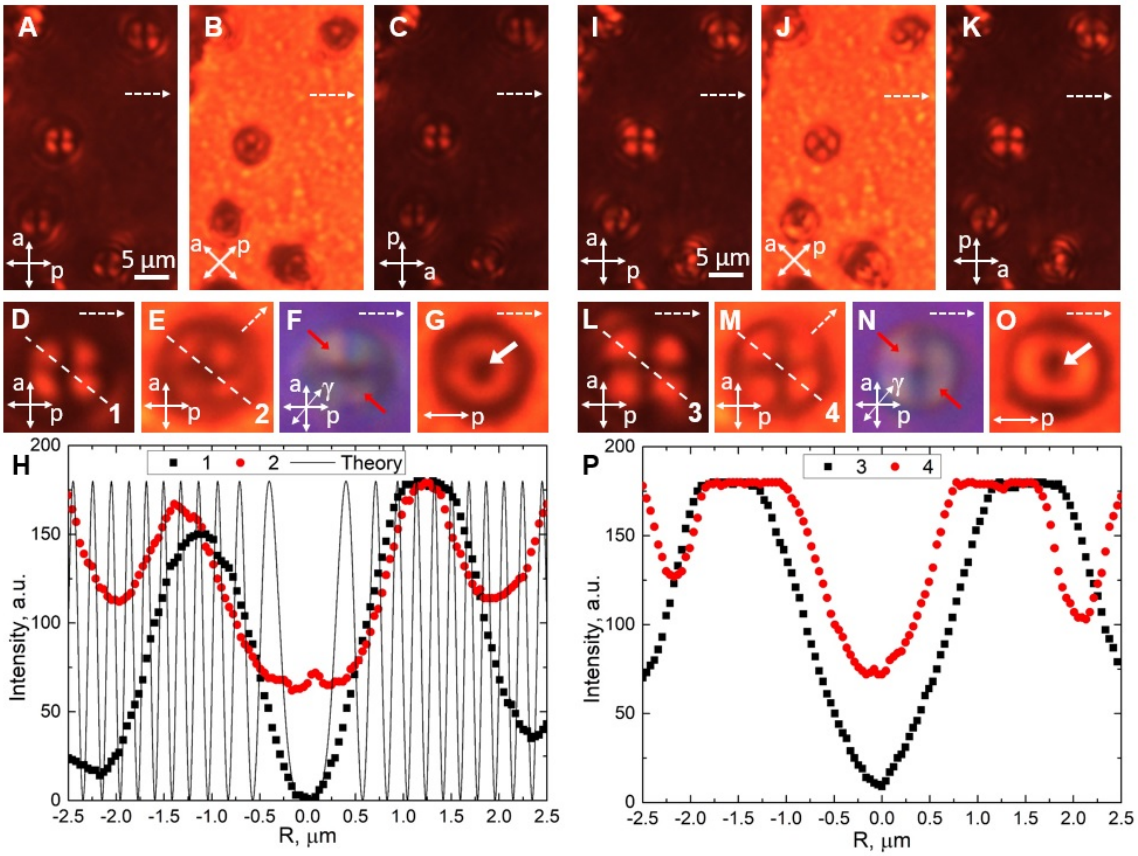

Fig. 2. POM images of the PET-8CB film (A-G, I-O) at different positions respectively to the polarizers and intensity profiles (H, P) along the dashed lines (1–4): nematic phase (A-H) at T = 36 °C, SmA phase (I-P) at T = 28 °C. Single dashed and bold (G, O) arrows indicate an optical axis of the film and the area with strong variations of the effective refractive index, respectively. Double headed arrows indicate directions of the polarizer (p) and analyzer (a), where γ is the slow axis of a full wave plate (F, N). Thin single red arrows show quadrants with a yellow color. Fitting parameters (H): σ = 12 [9], n_0 = 1.66, n_e = 1.52, d = 23 μm, R = 2.5 μm, λ = 650 nm

We also studied optical textures of 8CB in the smectic phase. At cooling nematic to SmA, we observed similar optical textures with a more uniform invariant cross and brighter areas in quadrants within the pores. Comparing the intensity profiles for nematic and SmA phases (Fig. 2, H,P), one sees an expansion of peaks and increasing of the light intensity respectively to the nematic phase as a result of higher order parameter of SmA. The presence of the wide black spot also shows the strong variation of the effective refractive index in the central region of pores for the SmA phase. It excludes formation of the chevron structure (CHV), which was observed at the X-ray study of 8CB within glass capillaries (d = 25 μm), treated by lecithin (provides weak homeotropic anchoring) [12]. For strong anchoring, which provides chromolan used in the present study, it was theoretically predicted SPR and smectic escaped radial (ESR) configurations (see [8]). For the SmA phase, only splay K_{11} elastic deformation is allowed whereas twist K_{22} and bend K_{33} deformations are prohibited. Therefore, the ESR configuration is more favorable than the SPR structure, which is energetically expensive and requires a line defect along the cylinder axis. Previously the ESR structure with SmA layers near the pore walls and melted core region was also observed in submicrometer pores of a diameter 0.2 μm (Anopore membranes) [10].

Conclusion

In summary, we studied optical textures and internal ordering of 8CB in deep nematic and SmA phases, confined to porous PET films at a propagation of the light along the pore's axis. The PET films with cylindrical pores of the diameter 5 μm were preliminary treated by chromolan to provide strong homeotropic anchoring at the pore walls. Contrary to different spatial ordering, both LC phases exhibited the similar cross like pattern and black spot in the center of pores, indicating the presence of a strong variation of the effective refractive index. Our observations indicate the presence of ER and SER configurations for nematic and SmA phases, respectively, but the ERPD and SPR configurations should not be also excluded. The additional study (X-ray, for example) is required to clarify internal ordering of 8CB in porous PET films. The presented data can be used in photonic LC applications.

Acknowledgements: *This work was supported by Ministry of Education and Science of Russian Federation, identification number – RFMEFI58316X0058.*

References

1. Urbanski M., Reyes C.G., Noh J., Sharma A., Geng Y., Subba Rao Jampani V., Lagerwall J.P. Liquid crystals in micron-scale droplets, shells and fibers. *J. Phys. Condens. Matter.,* 2017, **29** (13), 133003.
2. Carlton R.J., Hunter J.T., Miller D.S., Abbasi R, Mushenheim P.C., Tan L.N., Abbott N.L. Chemical and biological sensing using liquid crystals. *Liq. Cryst. Rev.,* 2013, **1** (1), 29–51.
3. Popov N., Smirnova A., Usol'tseva N., Popov P., Determination of concentrations of surface-active materials in aqueous solutions at different pH values using liquid crystals. *Liq. Cryst. and their Appl.,* 2017, **17** (1), 34–42.
4. Chigrinov V.G. Liquid crystal photonics. New York: Nova Science Publishers, 2014, 212 p.
5. Ito R., Kumagai T., Yoshida H., Takeya K., Ozaki M., Tonouchi M., Nose T. THz Nematic Liquid Crystal Devices Using Stacked Membrane Film Layers. *Mol. Cryst. Liq. Cryst.*, 2011, **543** (1), 77/[843]–84/[850].
6. Pasechnik S.V., Shmeliova D.V., Dubtsov A.V., Trifonov S.V., Chigrinov V.G. Electrically induced shear flows of liquid crystals confined to porous polymer films for THz applications. *Liq. Cryst. and their Appl.*, 2018, **18** (1), 79–83.
7. Kleman M., Lavrentovich O.D. Soft matter physics: an introduction. New York: Springer, 2003, 638 p.
8. Kralj S., Žumer S. Smectic-A structures in sub-micrometer cylindrical cavities. *Phys. Rev. E,* 1996*,* **54** (2), 1610–1617.
9. Ondris-Crawford R.J., Crawford G.P., Doane J.W., Zumer S., Vilfan M., Vilfan I.I. Surface molecular anchoring in microconfined liquid crystals near the nematic-smectic-A transition. *Phys. Rev. E*, 1993, **48**, 1998. **DOI**: 10.1103/PhysRevE.48.1998.
10. Iannacchione G., Finotello D. Confinement and orientational study at liquid crystal phase transitions. *Liq. Cryst.,* 1993, **14** (4), 1135–1142.
11. Kutnjak Ž., Kralj S., Lahajnar G., Žumer S. Calorimetric study of 8CB liquid crystal confined to controlled–pore glasses. *Phys. Rev.*, 2003, **68,** 021705.
12. Mang J.T., Sakamoto K., Kumar S. Smectic Layer Orientation in Confined Geometries. *Mol. Cyst. Liq. Cryst.*, 1992, **223** (1), 133–142.
13. Maksimochkin G.I., Shmeliova D.V., Pasechnik S.V., Dubtsov A.V., Semina O.A., Kralj S. Orientational fluctuations and phase transitions in 8CB confined by cylindrical pores of the PET film. *Phase Transitions,* 2016, **89**, 846–855.

14. Scudieri F. Cylindrically aligned liquid crystals: an interferometric analysis. *Appl. Optics*, 1979, **18** (9), 1455–1459.
15. Crawford G.P., Allender D.W., Doane J.W. Surface elastic and molecular–anchoring properties of nematic liquid crystals confined to cylindrical cavities. *Phys. Rev.*, 1992, **45**, 8693–8708.

Appendix

For the case of ER configuration, variation of the angle within the cylindrical pore describes by the following equation:

$$ctg(\theta/2) = \sqrt{\frac{\sigma+1}{\sigma-1}}(R/r), \quad (1)$$

where

$$\sigma = \frac{RW}{K_{11}} + \frac{K_{24}}{K_{11}} - 1 \quad (2)$$

is a dimensionless surface parameter [15]. It leads to the next expression:

$$\sin^2\theta = \frac{4ctg^2(\theta/2)}{[1+ctg^2(\theta/2)]^2} = \frac{4c^2(r/R)^2}{[(r/R)^2+c^2]^2}, \quad (3)$$

where

$$c = \left((\sigma+1)/(\sigma-1)\right)^{1/2}. \quad (4)$$

The obtained expressions can be used to analyze the image of the pore in crossed polarizers. The optical phase difference can be expressed as:

$$\delta(r) = (2\pi/\lambda)\Delta nd\sin^2\theta(r). \quad (5)$$

The phase delay defines polarized light intensity passing an LC layer along pores:

$$I(r) = I_0\sin^2\left(\delta(r)/2\right). \quad (6)$$

Поступила в редакцию 19.11.2018 г.
Received 19 November 2018